Functional analysis of skunk cabbage alternative oxidase in human cells

ヒト細胞発現系を用いたザゼンソウシアン耐性呼吸酵素の機能解析

Kazushige Matsukawa

United Graduate School of Agricultural Science

Iwate University

Morioka

Iwate

Japan

Contents

Introduction

Alternative oxidase (AOX) is a mitochondrial enzyme that plays a central role in cyanide-insensitive respiration in eukaryotic taxa excluding mammals [1]. AOX acts as an alternative terminal oxidase in the electron transfer chain (ETC). It catalyzes the oxidation of ubiquinol, reducing molecular oxygen to water. Therefore, it is believed that as a result of bypassing two proton translocation sites in the cytochrome respiratory pathway (complexes III and IV), the redox energy which is not conserved for ATP synthesis is released as heat [2]. In fact, the massive respiratory burst that occurs during anthesis in thermogenic plants, such as the arum lily family (Araceae), has been attributed to the upregulation of a cyanide-resistant alternative respiratory pathway [2-6]. Separate from thermogenic plants, previous studies in non-thermogenic plants have shown that the presence of AOX can prevent the prolonged reduction of ubiquinone, a status that would otherwise lead to reactive oxygen species (ROS) production, while allowing continuous operation of the ETC and the tricarboxylic acid cycle (TCA) [3,7,8].

In many organisms, ROS participate in cell signaling or injury and most of the intracellularly produced ROS originates in the mitochondrial ETC, in particular from complexes I and III [9,10]. In humans, uncontrolled increases in cellular ROS levels are thought to contribute to a wide range of pathological conditions, including aging, cancer, metabolic syndrome, and neurodegenerative and mitochondrial diseases [11-13]. Consequently, the quenching of excessive ROS should be one of the primary goals of therapies aimed at relieving the

harmful consequences of pathological respiratory chain deficiency.

It has been shown that human cells can exhibit cyanide-resistant respiration through the allotopic expression of an animal *AOX* gene from ascidian *Ciona intestinalis* [13]. It has also been shown that AOX expression abrogated the apparent induction of superoxide dismutase (SOD) activity caused by antimycin A (AA), a mitochondrial complex III inhibitor [13]. Nevertheless, it is not clear whether mitochondrial AOX is capable of preventing the increase in ROS production provoked by AA in human cells.

In the present study, we show that plant AOX from the thermogenic skunk cabbage *Symplocarpus renifolius* [14] can be functionally expressed in the HeLa cell line and that AOX expression lowers AA-initiated ROS production. Interestingly, this AOX protection against mitochondrial oxidative stress was observed in cells grown in galactose medium with active respiration. Our findings should be helpful for future investigation of dysfunctions in cytochrome respiration underlying various mitochondrial diseases in human cells.

Materials and methods

Cell culture conditions

The HeLa cell line, originally derived from a human cervical carcinoma, were grown in glucose- or galactose-containing media and kept in a humidified atmosphere with 5% (v/v) CO_2 at 37°C. The glucose medium consisted of glucose-free Dulbecco's modified Eagle's medium (DMEM, Invitrogen Inc., Carlsbad, CA, U.S.A.) supplemented with 5.5 mM glucose, 2 mM glutamine (6 mM final), 5 mM Hepes, 1 mM potassium pyruvate, and 10% (v/v) heat-inactivated fetal calf serum (FCS, CELLect, MP Biomedicals Inc., Aurora, OH, U.S.A.). The galactose medium consisted of glucose-free DMEM (Invitrogen) supplemented with 10 mM galactose, 2 mM glutamine (6 mM final), 5 mM Hepes, 1 mM potassium pyruvate, and 10% (v/v) FCS.

Plasmid construction and transfection

For transient transfection, a sequence encoding the putative mature AOX protein was obtained from a full-length *Symplocarpus renifolius* cDNA [14] (*SrAOX*, DDBJ Accession No. AB183695). This sequence was subcloned into the pShooter pCMV/myc/mito plasmid (Invitrogen) containing the human COX VIII mitochondrial targeting signal without the myc epitope. PCR was performed using full-length AOX as a template and KOD-plus DNA polymerase (Toyobo Inc., Tokyo, Japan) for 30 cycles at 95°C for 1 min and 68°C for 2 min. The following oligonucleotides were used to obtain the fragment encoding the putative mature AOX containing a *Pst*I restriction

site: forward, MTSaox_F1 (23-mer): 5'-ACTGCAGTCCGTGCCGGCCGCC C-3'; reverse, Sraox_full_R1 (22-mer): 5'-ATAAGTGGTACCCGAGCGGCG C-3'. The PCR product was subcloned into the pUC118-blunt vector (Takara Bio Inc., Tokyo, Japan) and the *Pst*I fragment containing the mature AOX was removed by *Pst*I digestion and subcloned into the *Pst*I site of the pShooter vector. The resultant plasmid was confirmed by sequencing and designated AOX. To create a mutant AOX protein with a malfunctioning di-iron center, the Glu-217 codon (GAG) of the AOX cDNA was converted to alanine (GCC) using a QuickChange Site-Directed Mutagenesis Kit (Strategene Inc., La Jolla, CA, U.S.A.). PCR was performed using AOX subcloned into the pShooter vector as a template and KOD-plus DNA polymerase for 30 cycles at 95°C for 1 min and 68°C for 2 min. The following mutagenic oligonucleotides were used for amplification. Forward, E217A (Sr)-F (36-mer): 5'-GAATGAGGCCGAGAACGCCAGGATGCACCTGATGA C-3'; reverse, E217A (Sr)-R (36-mer): 5'-GTCATCAGGTGCATCCTGGCGT TCTCGGCCTCATTC-3'. The resultant plasmid was verified by sequencing and designated E217A. For all transfection experiments, HeLa cells were plated at 2.5×10^6 cells per 10 cm dish. Either AOX, E217A, or the corresponding empty vector plasmid (control) was transfected into HeLa cells using Lipofectamine™ 2000 (Invitrogen) at a 4:1 molar ratio along with a nuclear localizing red fluorescent protein pDsRed2-Nuc (BD Biosciences Clontech Inc., San Jose, CA, U.S.A.) as a transgene marker.

Subcellular localization and Western blotting

Subcellular localization of transfected gene product was determined using a Subcellular Proteome Extraction Kit (Calbiochem Inc., San Diego, CA, U.S.A.). Twenty-four hours after transfection, HeLa cells were trypsinized and fractionated according to the manufacturer's protocol. The protein concentration was measured using the Bradford method (Bio-Rad Laboratories Inc., Hercules, CA, U.S.A.) with bovine serum albumin (BSA) as a standard. Each sample (20 μg) was fractionated by SDS-PAGE on a 12.5% acrylamide gel and transferred onto PVDF membranes (Immobilon-P; Millipore Inc., Bedford, MA, U.S.A.) using a semi-dry blotting system (HorizBlot; Atto Inc., Tokyo, Japan). Prestained protein markers (11-170 kDa; Fermentas Inc., Burlington, Ontario, Canada) were used for molecular mass estimation. The membranes were incubated for 1 h at room temperature in 5% (w/v) skim milk in Tris-buffered saline (137 mM NaCl, 2.68 mM KCl, and 25 mM Tris/HCl, pH7.4) containing 0.1% (v/v) Tween 20 (TBS-T), and then overnight at 4°C in TBS-T with primary antibodies against AOX (mouse monoclonal antibody generated from *Sauromatum guttatum* AOX [15]), μ-calpain (mouse monoclonal antibody; Sigma-Aldrich Inc., St. Louis, MO, U.S.A.), and Complex III core 2 subunit (CIII; mouse monoclonal antibody; Invitrogen). Detection was achieved using a horseradish peroxidase-conjugated secondary antibody (anti-mouse IgG; Pierce Biotechnology Inc., Rockford, IL, U.S.A.) and SuperSignal West Femto Maximum Sensitivity Substrate (Pierce Biotechnology) and a digital image analyzer (Light-Capture AE6955, Atto).

Isolation of mitochondria

HeLa cell mitochondria were prepared as described previously [16] with minor modifications. Briefly, cells were harvested by trypsin-EDTA treatment from a total of 30 10 cm culture dishes. The cells were washed with phosphate-buffered saline (PBS) and centrifuged for 5 min at 200 × *g*. The pellet was resuspended in 10 ml of "H-medium" (210 mM mannitol, 70 mM sucrose, 0.5% (w/v) defatted bovine serum albumin (BSA), and 5 mM Hepes/KOH, pH 7.2) containing 1 mM EGTA. These cells were then homogenized using a Potter-Elvehjem tissue grinder (Alcan Packaging Inc., Pennsauken, NJ, U.S.A.). After centrifugation at 800 × *g* for 15 min, all supernatants were further centrifuged at 10000 × *g* for 30 min (mitochondria in pellet). The mitochondrial fractions were then resuspended in 500 μl of "H-medium" and used for further respiration analyses. The yield of a typical preparation was approximately 0.8 mg of mitochondrial protein per 10^8 HeLa cells.

Measurements of oxygen consumption

Cells were trypsinized and the number of living cells was determined using a trypan blue dye exclusion assay [17]. Endogenous whole cell respiration was measured using a Clark-type electrode (Oxy1, Hansatech Instrument Inc., King's Lynn, Norfolk, U.K.) at 37°C in individual growth media as mentioned above. Oxygen consumption by mitochondrial isolates was measured according to a previously described method [16] using a Clark-type electrode (Oxy1) at 37°C in an incubation medium containing 130 mM KCl, 2 mM KH_2PO_4, 2 mM $MgCl_2$, and 10 mM Mops/NaOH (pH 7.2). The oxygen concentration in

air-saturated water at 37°C was estimated to be 200 μM in each experiment.

Gas chromatography-mass spectrometry

Measurements of intracellular organic acids were performed as described previously [18] with minor modifications. Briefly, 24 h after transfection with the control, AOX, or E217A plasmid, cells were trypsinized and washed in PBS 3 times, and stored at -80°C until analysis. Cells in the mock experiment were not transfected and were processed as described. Aliquots of frozen cells were suspended in 2% (w/v) sulfosalicylic acid (250 μl), and disrupted by sonication (VCX500, Sonics & Materials Inc., Newtown, CT, U.S.A.) followed by 20-min of vortex. Cellular debris was removed by centrifugation at 15300 × *g* for 10 min, and the supernatant was filtrated through a membrane filter (0.45 μm pore size, GHP Nanosep MF Centrifugal Device, Pall Life Sciences Inc., Ann Arbor, MI, U.S.A.). After subsequent centrifugation at 9100 × *g* for 5 min, the supernatant was mixed with 5% aqueous hydroxylamine hydrochloride (125 μl) and 2.5N-NaOH (50 μl) and reacted at 30°C for 60 min. Then 43.8 μl of 6N-HCl was further added to the sample and extracted with 750 μl of ethyl acetate. After subsequent centrifugation at 9100 × *g* for 3 min, the upper ethyl-acetate layer was transferred to a 2 ml-tube containing 0.5 g of sodium sulfate, mixed and centrifugated again at 9100 × *g* for 5 min. The upper layer was air dried at 60°C, and the residue was resuspended with 100 μl mixture of N,O-bis (trimethylsilyl) trifluoroacetamide (BSTFA) and trimethylchlorosilane (TMCS) (10:1, v/v), and reacted at 80°C for 30 min. The trimethylsilylated sample was subjected to GC/MS analysis (GCMS-QP2010, Shimadzu Inc., Kyoto, Japan) with a HP-50+

column (Agilent Technologies Inc., Santa Clara, CA, U.S.A.) according to the manufacturer's instructions.

Measurement of ROS production by flow cytometry

Intracellular ROS generation was detected by means of an oxidation-sensitive fluorescent probe dye [5-(and-6)-chloromethyl-2',7'-dichlorodihydrofluorescein diacetate acetyl ester (CM-H_2DCFDA)] (Invitrogen), as a cell-permeable indicator of ROS and in particular H_2O_2. This fluorescent probe dye allows for covalent attachment to intracellular components once it is deacetylated intracellularly by a non-esterase, permitting longer retention within the cell. The deacetylated H_2DCF (2',7'-dichlorofluorescein) is non-fluorescent until oxidation occurs within the cell. Twenty-four hours after transfection, cells were trypsinized and transferred into fresh growth medium. Transfected cells were incubated with 5 μM CM-H_2DCFDA for 30 min at 37°C, and then batches of cells were treated with various concentrations of AA (Sigma-Aldrich) for 30 min at 37°C. After washing with phosphate-buffered saline (PBS), the DCF fluorescence intensity of DsRed2-nuc positive cells was immediately analyzed by flow cytometry (FACScan; Becton, Dickinson & Company Inc., Franklin Lakes, NJ, U.S.A.) according to the manufacturer's instructions. For each experiment, 10000 DsRed2-nuc positive events were collected and analyzed.

Statistical analysis

The Student *t*-test was used for statistical analysis. Values are

expressed as mean ± S.E.M. P values < 0.05 were considered statistically significant.

Results

Both AOX and E217A are expressed as non-covalently associated dimers in the mitochondria of HeLa cells grown in glucose and galactose medium

To perform the functional analysis of *Symplocarpus* AOX in human cells, we constructed an AOX plasmid, which encoded the mature form of *Symplocarpus* AOX fused to a human cytochrome c oxidase (COX) VIII mitochondrial targeting signal (MTS) [19] at its N terminus (Fig. 1), and an E217A plasmid harboring a malfunctioning di-iron center generated by site-directed substitution of Glu-217 with Ala (Fig. 1) [20-22]. After transfection, cell proteins were immunoblotted under non-reducing conditions using an AOX monoclonal antibody raised against *S. guttatum* AOX [15]. A total of 24 h after the transfection with the control, AOX, or E217A plasmid, cytosolic and mitochondrial fractions were isolated from cells grown either in glucose or galactose medium. Fig. 2 shows that AOX proteins co-fractionated with the mitochondrial marker protein complex III subunit core 2. Furthermore, both of the mitochondrially targeted AOX proteins were predominantly expressed as a mature form, with a predicted molecular mass of 32 kDa, and there were fewer signals for the oxidized dimer in both mitochondrial fractions. The AOX protein with the extra MTS sequence was weakly detected in E217A-transfected mitochondria (Fig. 2). In both cell growth mediums, E217A showed slightly more accumulation in the mitochondrial fraction than did AOX (Fig. 2).

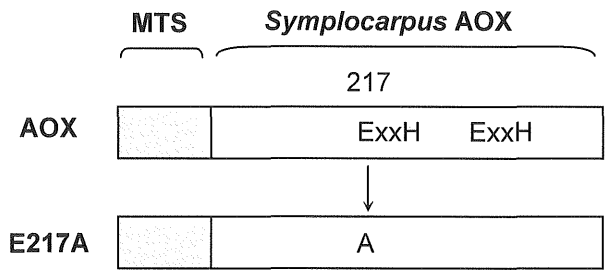

Figure 1. Schematic representation of AOX and E217A constructs. Two highly conserved iron-binding motifs (EXXH) found in AOX species are shown. In E217A, Glu-217 of *Symplocarpus* AOX was replaced by Ala. MTS; mitochondrial targeting signal of human COX VIII.

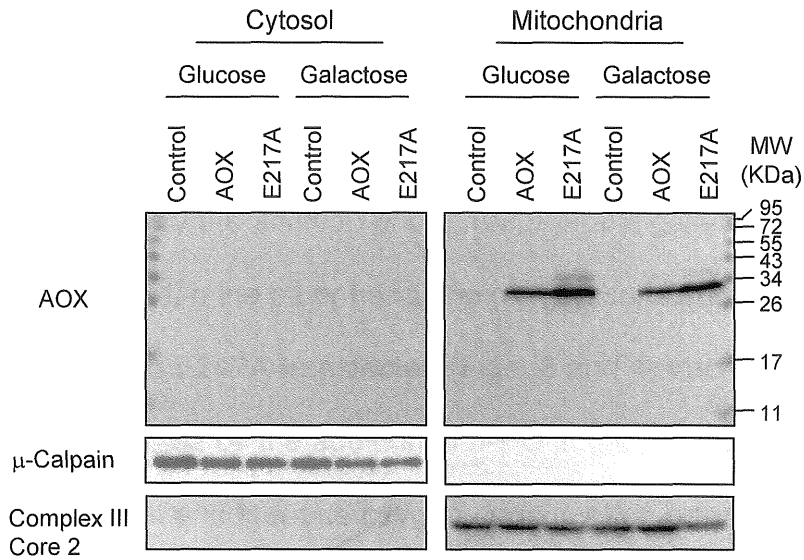

Figure 2. Expression and subcellular localization of AOX and E217A in HeLa cells grown in glucose or galactose medium. Cytosolic and mitochondrial fractions (20 μg) from transfected cells were separated on 12.5 % SDS-PAGE under non-reducing conditions and immunoblotted with the AOA monoclonal antibody against *S. guttatum* AOX [15], anti-μ-calpain (cytosolic marker), or anti-complex III core 2 subunit (mitochondrial marker). The positions of the molecular mass standards are indicated on the right of the panel. Data are representative results from two independent experiments.

AOX, but not E217A, confers cyanide-resistant respiration to HeLa cells

To determine whether AOX confers cyanide-resistant respiration to human cells, we measured rates of endogenous cellular oxygen consumption at 37°C in a buffer lacking pyruvate. As shown in Fig. 3 (for glucose-grown) and Fig.4 (for galactose-grown), 24 h after transfection with AOX (Figs. 3 and 4, trace b), the cells exhibited substantial resistance to 1 mM cyanide and were virtually completely inhibited by the addition of 0.1 mM *n*-propyl gallate (*n*-PG), a specific inhibitor of AOX [23]. On the other hand, the oxygen consumption of control (Figs. 3 and 4, trace a) and E217A-transfected (Figs. 3 and 4, trace c) HeLa cells was not significantly affected by the addition of *n*-PG in the presence of cyanide. The percentages of basal endogenous oxygen consumption rates were 34.3 ± 4.4% and 28.6 ± 4.4% in glucose- and galactose-grown cells, respectively (Fig. 5, black bar). Addition of 1 mM pyruvate enhanced the respiration rate of AOX-expressing cells in the presence of cyanide (Figs. 3 and 4, trace b). Addition of 1 mM pyruvate increased cyanide-resistant respiration more efficiently in AOX-expressing cells grown in galactose medium than in glucose medium (fold change of cyanide-resistant respiration by the addition of pyruvate was 1.5 ± 0.2-fold in glucose and 1.9 ± 0.1-fold in galactose, Fig. 5, black bar). Our recent studies have shown that *Symplocarpus* AOX is pyruvate-sensitive and that the addition of 1 mM pyruvate induces an approximately two fold increase in cyanide-resistant respiration [14].

To further assess the effects of 1 mM pyruvate on cyanide-insensitive respiration in AOX-expressing mitochondria isolated from glucose-grown cells, we measured oxygen consumption at 37°C using mitochondria from cells

transfected with the control plasmid, AOX, or E217A. As shown in Fig. 6, in cells transfected with control (trace a) or E217A (trace c), addition of 0.5 mM KCN caused a dramatic decrease in respiration. However, progressive addition of 0.5 mM KCN to AOX-expressing mitochondria (trace b) resulted in significant cyanide-resistant and *n*-PG-sensitive respiration (Fig. 6). Moreover, addition of pyruvate (1 mM), but not α-ketoglutarate (1 mM) caused a 2.3 ± 0.2-fold (n = 3) increase in cyanide-insensitive respiration (Fig. 7, traces a and b). It should be noted that there was no significant effect of heterologous expression of AOX on the basal and state 2 respirations (Table 1).

Glucose-grown

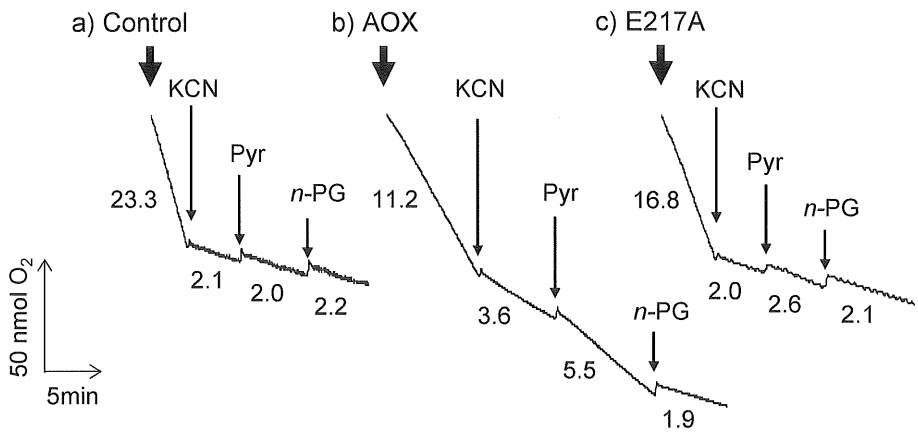

Figure 3. HeLa cell endogenous oxygen consumption. Glucose-grown cells were transfected with the empty vector (control), AOX, or E217A, and cellular oxygen consumptions were measured with buffers deprived of pyruvate (see Materials and methods section) at 37°C. The numbers of living cells, assessed using the trypan blue dye exclusion assay, were as follows: 10.4×10^6 (control), 7.0×10^6 (AOX), and 6.4×10^6 (E217A) under glucose-grown conditions. The graphed data are representative of three different experiments. Numbers along the traces represent a typical value from three independent experiments (nmol O_2/min per dish). KCN, 1 mM potassium cyanide; Pyr, 1 mM potassium pyruvate; *n*-PG, 0.1 mM *n*-propyl gallate.

Galactose-grown

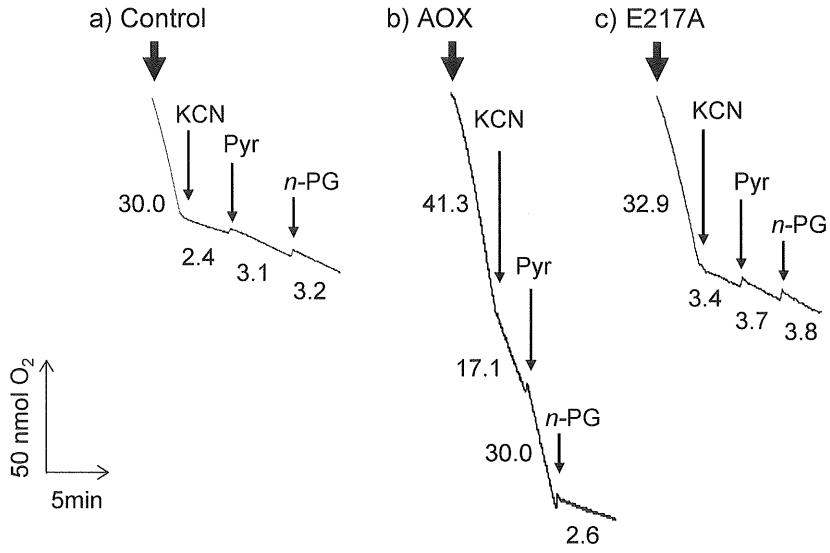

Figure 4. HeLa cell endogenous oxygen consumption. galactose-grown cells were transfected with the empty vector (control), AOX, or E217A, and cellular oxygen consumptions were measured with buffers deprived of pyruvate (see Materials and methods section) at 37°C. The numbers of living cells, assessed using the trypan blue dye exclusion assay, were as follows: 8.9×10^6 (control), 11.3×10^6 (AOX), 12.6×10^6 (E217A) under galactose-grown conditions. The graphed data are representative of three different experiments. Numbers along the traces represent a typical value from three independent experiments (nmol O_2/min per dish). KCN, 1 mM potassium cyanide; Pyr, 1 mM potassium pyruvate; *n*-PG, 0.1 mM *n*-propyl gallate.

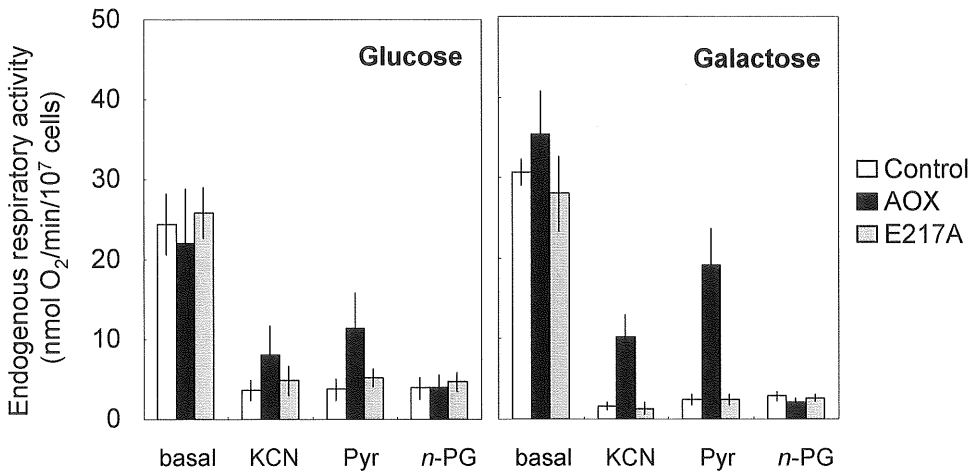

Figure 5. HeLa cell endogenous oxygen consumption. Summary of HeLa cell oxygen consumption in the medium containing glucose (left panel) or galactose (right panel). The data represent the mean ± S.E.M. of three independent experiments (nmol O_2 /min per 10^7 cells). KCN, 1 mM potassium cyanide; Pyr, 1 mM potassium pyruvate; *n*-PG, 0.1 mM *n*-propyl gallate.

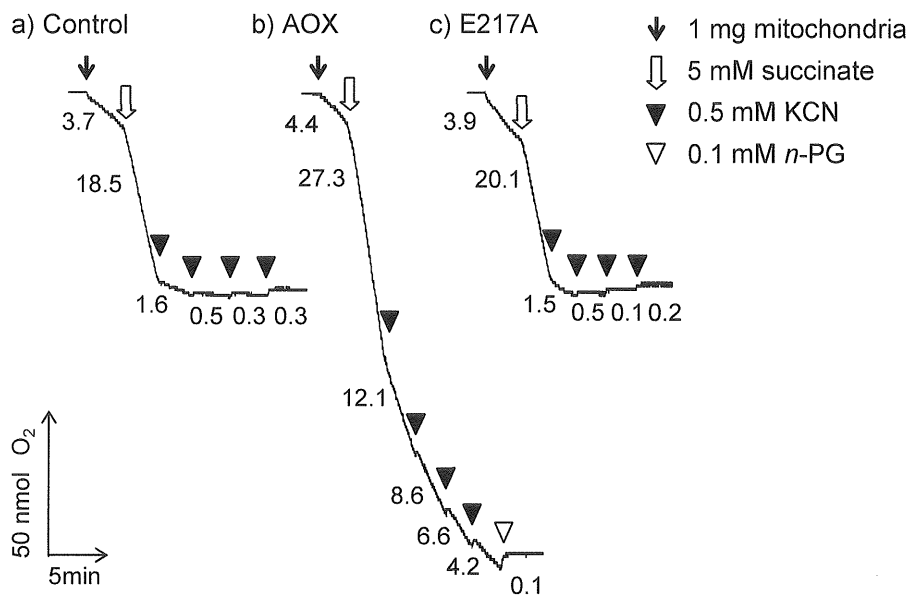

Figure 6. Oxygen consumption of mitochondrial isolates from HeLa cells. Glucose-grown cells were transfected with control (empty vector; trace a), AOX (b), and E217A (c). The oxygen consumption rate of each mitochondrial isolate was measured at 37°C in incubation medium with additions as indicated by the specific arrows. In traces a-c, 1 mg of mitochondrial protein was used. Numbers along the traces represent typical values from three different preparations (nmol O_2/min).

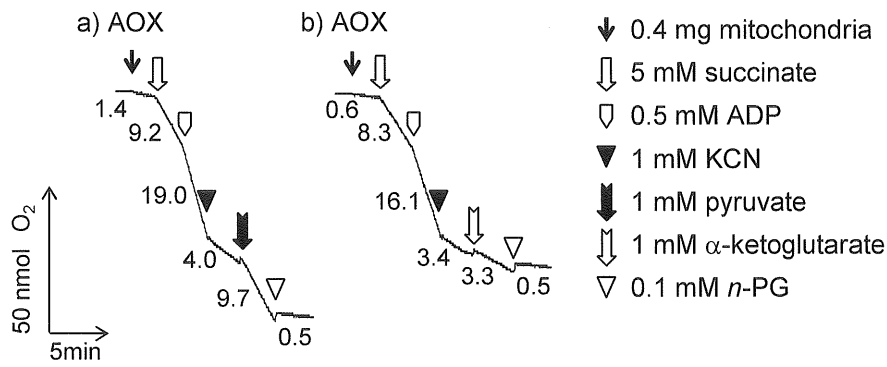

Figure 7. Oxygen consumption of mitochondrial isolates from HeLa cells. Glucose-grown cells were transfected with AOX (a and b). The oxygen consumption rate of each mitochondrial isolate was measured at 37°C in incubation medium with additions as indicated by the specific arrows. In traces a and b, 0.4 mg of mitochondrial protein was used. Numbers along the traces represent typical values from three different preparations (nmol O_2/min).

Table 1
Respiratory activities of mitochondria isolated from AOX and E217A-transefected HeLa cells

	Basal	5 mM succinate	0.5 mM KCN	1 mM KCN	1.5 mM KCN	2 mM KCN	0.1 mM *n*-PG
Control	8.5±5.1	27.1±8.8	3.7±1.9	1.5±1.0	1.1±0.7	0.9±0.5	ND
AOX	6.5±3.9	28.3±1.3	12.7±0.9*	8.8±0.3*	6.7±0.3*	4.3±0.1*	0.1±0.1
E217A	3.2±0.9	17.1±2.9	1.5±0.3	0.6±0.2	0.5±0.3	0.5±0.3	ND

Cyanide-insensitive respiratory activity was determined by the sequential addition of 5 mM succinate, 0.5 mM KCN, and 0.1 mM *n*-propyl gallate (*n*-PG). The rates of oxygen consumption (nmole O_2/min/mg of protein) are the mean ± S.D. (n = 3). * Indicates significantly different (t-test; $p<0.05$).

Intracellular pyruvate content in glucose-grown HeLa cells is higher than that of galactose-grown cells

Because pyruvate was less effective at stimulating AOX activity in glucose-grown cells, we next determined whether growth conditions (glucose or galactose medium) altered the levels of intracellular organic acids, in particular pyruvate. Quantitative gas chromatography/mass spectrometry (GC/MS) measurements were performed for eight different organic acids and showed that the intracellular pyruvate content of the glucose-grown cells was approximately four times higher than those detected in galactose-grown cells (Fig. 8). Moreover, AOX expression did not significantly affect the intracellular pools of other organic acids of cells grown in either growth medium (Fig. 8).

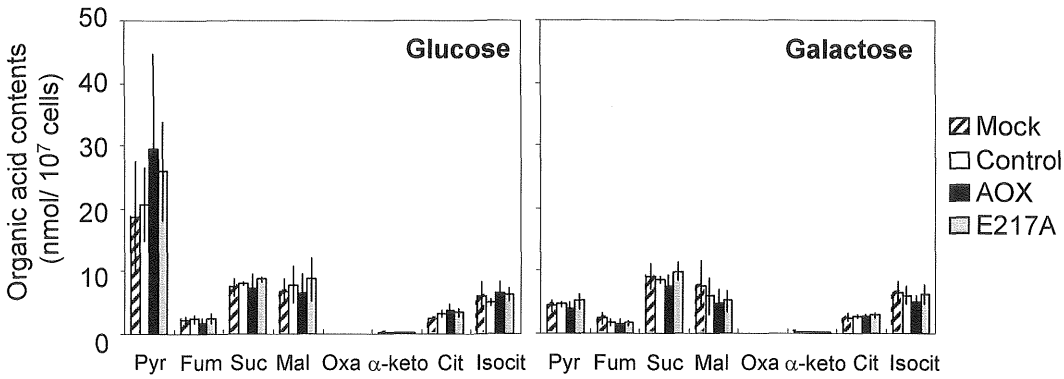

Figure 8. The levels of organic acids within cells transfected with mock-treatment, control (empty vector), AOX, and E217A were determined by GC/MS analysis. Pyr, pyruvate; Fum, fumarate; Suc, succinate; Mal, malate; Oxa, oxaloacetate; α-keto, α-ketoglutarate; Cit, citrate; Isocit, isocitrate. The data represent the mean ± S.E.M. of three independent experiments.

AOX, but not E217A, diminishes AA-induced ROS production in galactose-grown HeLa cells

To determine the effects of AA on oxygen consumption and ROS production in glucose- and galactose-grown cells, cellular ROS generation was measured using the DCF fluorescence intensity and flow cytometry. As shown in Fig. 9, oxygen consumption was severely inhibited in the presence of lower concentration of AA in both glucose- and galactose-grown cells (0.01 μg/ml). Addition of KCN and *n*-PG had no detectable effect on oxygen consumption, since these cells were not transfected with an AOX-expressing plasmid. ROS production, monitored by DCF fluorescence intensity, was significantly increased in galactose-grown cells incubated with AA (0.01, 0.02, and 0.2 μg/ml) (Fig. 10).

We next determined the effect of AA-induced mitochondrial ROS production on AOX-expressing cells grown either in glucose or galactose media. If the AOX is sufficiently functional, the presence of AOX can prevent ROS generation by bypassing the AA-induced blockade of electron flow. No significant increase in DCF fluorescence was observed in glucose-grown cells (Fig. 11, left panel). However, in galactose-grown cells, cellular ROS production was increased in both control and E217A cells in the presence of AA (0.01 μg/ml) (Fig. 11, right panel). On the contrary, AOX-expressing cells treated with AA (0.01 μg/ml) showed significant inhibition of ROS formation and DCF fluorescence levels were similar to those of untreated cells (control, AOX, or E217A) (Fig. 11, right panel). ROS production in AOX-expressing cells was again observed following cell treatment with 0.1 mM *n*-PG (Fig. 11, right panel).

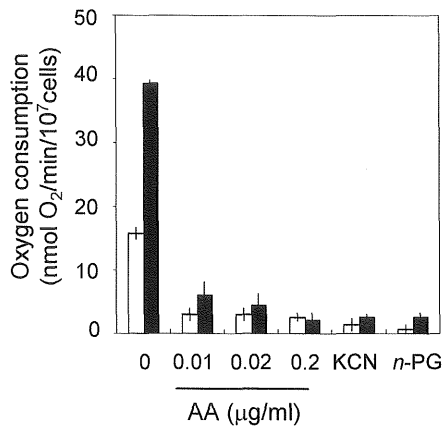

Figure 9. Effects of antimycin A (AA) on oxygen consumption in glucose- or galactose- grown HeLa cells. The oxygen consumption of whole cells grown in either glucose or galactose was measured following treatment with various concentrations of AA at 37°C. After treatment with AA, KCN (1 mM potassium cyanide) and *n*-PG (0.1 mM *n*-propyl gallate) were sequentially added to the media and oxygen consumption was measured. Open and filled bars denote glucose- and galactose-grown cells, respectively. Data from a representative experiment are shown and are the mean ± S.E.M. of triplicate determinations from three independent experiments.

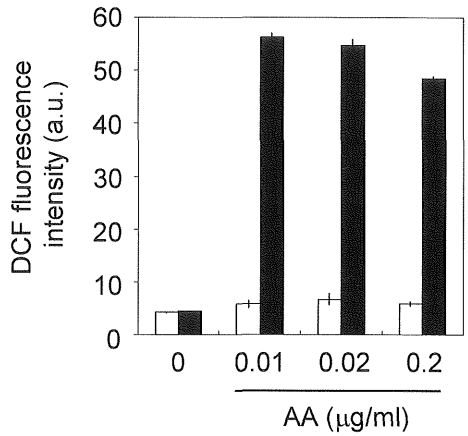

Figure 10. Antimycin A (AA)-induced reactive oxygen species (ROS) production in cells grown in media containing glucose or galactose. Cells were incubated with 5 μM CM-H_2DCFDA for 30 min at 37°C, treated with various concentrations of AA for additional 30 min at 37°C, and analyzed by flow cytometry. Open and filled bars denote glucose- and galactose-grown cells, respectively. Data from a representative experiment are shown and are the mean ± S.E.M. of triplicate determinations from three independent experiments.

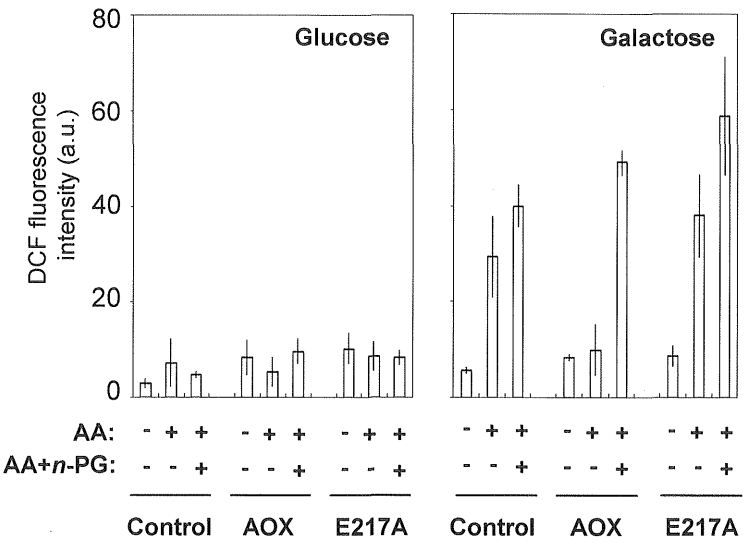

Figure 11. Effects of antimycin A (AA) on AOX-expressing glucose- or galactose-grown cells. After 24 h of transfection with vector alone (control), AOX, or E217A, the cells were treated with 5 μM CM-H_2DCFDA for 30 min at 37°C. Cells were further incubated with AA (0.01 μg/ml) for 30 min at 37°C and analyzed by flow cytometry. Data from a representative experiment are shown and are the mean ± S.E.M. of triplicate determinations from three independent experiments.

Discussion

It was recently reported that ascidian AOX from *C. intestinalis* could be expressed in human cells and that it conferred mitochondrial cyanide resistance [13]. However, the authors concluded that the expression of the plant AOX in mammalian cells was unsuccessful due to uncontrolled lethality in the AOX-expressing cells [13]. Thus, although the significance of the AOX protein in mitochondrial metabolism has been extensively studied in higher plants, no functional analyses of plant AOXs in mammalian cells have been reported.

Here I demonstrate that plant *Symplocarpus* AOX can be successfully expressed in human cells, and that it confers a cyanide-resistant respiration pathway to human mitochondria. In addition, we show that *Symplocarpus* AOX clearly mitigates AA-induced ROS generation in mammalian cells. Interestingly, this AOX protective effect against AA-induced ROS formation was observed only in cells grown in galactose medium with more active respiration.

In general, plant AOX activity is governed by two post-translational mechanisms which involve the redox status of the enzyme (either non-covalently or covalently associated dimer) and allosteric modification of the reduced active enzyme via α-keto acids such as pyruvate [24]. AOX from both fungi and protozoa appear to exist as non-covalently associated dimers that are not regulated by the redox status of the enzyme. Instead, their activity is modulated by purine nucleotides such as ADP, AMP, and GMP, but not by α-keto acids [25-27]. In fact, ascidian AOX also does not possess a regulatory cysteine residue which plays an important role in the formation of a thiohemiacetal bond

with pyruvate [24], although cyanide-insensitive respiration in the AOX-expressing cells was slightly activated by addition of 10 mM pyruvate [13]. Our recent studies have shown that *Symplocarpus* AOX is specifically stimulated by pyruvate and exists as a non-covalently associated dimer *in vivo* [5, 14]. In accordance with this status, my current results also show that *Symplocarpus* AOX exists predominantly as a reduced, non-covalently-associated dimer (Fig. 2) and that appears to be sensitive to pyruvate and is not stimulated by α–ketoglutarate (Fig. 7).

Interestingly, cellular cyanide-resistant respiration was more effectively activated by the addition of 1 mM pyruvate in galactose-grown cells than in glucose-grown cells (Fig. 5, black bar). GC/MS analyses showed that the intracellular pyruvate pool in galactose-grown cells was apparently smaller than in glucose-grown cells (Fig. 8), suggesting that cyanide-resistant respiration may be more effectively activated by exogenous pyruvate in galactose-grown cells. It was recently reported that a switch from the M1 to the M2 isoform of pyruvate kinase in tumor cells resulted in an increase of pyruvate and lactate levels with reduced oxygen consumption of the cells. Therefore, it is probable that pyruvate kinase M2, which is reported to be mainly expressed in glucose-grown HeLa cells [28], contributes to the increased pyruvate levels observed in these cells.

It has been suggested that ascidian AOX is also protective against AA-induced ROS formation in glucose-grown human embryonic kidney (HEK) 293T cells based on an apparent decrease in SOD activity after incubation with 60 μM AA for 16 h [13]. However, these observations are complicated by the possibility of up-regulation of other ROS detoxification enzymes such as catalase

and thioredoxin reductase [29]. Recent studies have also shown that higher concentrations of AA can bind not only cytochrome complex III at the Qi site, but also to the antioxidant protein Bcl-2 via its interaction with BH3 domains [30-32]. Thus, the current study using lower AA concentrations (0.01 μg/ml or 18.2 nM) and shorter periods of exposure (30 min) is the first report demonstrating that AOX plays a role in the prevention of ROS production in mammalian cells by direct measurement of AA-inducible ROS formation within the cells.

An intriguing question is why less ROS production was observed in AA-treated cells grown in glucose medium (Figs. 10 and 11). The Warburg effect [33], which is known to repress mitochondrial respiration in glucose-grown cells (Fig. 9), may be involved in this phenomenon. In accordance with this possibility, Wiesner and colleagues have shown that the combination of the mitochondrial uncoupler carbonyl cyanide m-chlorophenyl hydrazone (CCCP) with AA caused a significant elevation of ROS in glucose-grown HeLa cells, while AA alone had much smaller effects [34]. Another possible explanation is the involvement of glucose metabolism, which could potentially affect antioxidant activity within the cells. For example, glucose can induce SOD activity [35], produce excess pyruvate as an antioxidant (Fig. 8) [36], and produce intermediates of the pentose phosphate pathway, in which an antioxidant of the glutathione redox cycle, NADPH, is generated [37].

Rustin and colleagues noted that ascidian AOX was inactive under normal culture conditions [13], and they suggested that if AOX remains in a constitutively active form (as a non-covalently associated dimer), it would be detrimental to cell growth because of the associated decrease in ATP. Our

results also show that despite the expression of AOX as a non-covalently associated dimer, the rate of basal oxygen consumption of AOX-expressing cells was not significantly enhanced either in glucose- or galactose-grown cells (Fig. 5). These results suggest that *Symplocarpus* AOX may have been less active under my culture conditions and that it was activated only under specific conditions when complex III was inhibited by AA.

Mitochondrial diseases have been generally attributed to dysfunctions in the cytochrome pathway, resulting in damage to organs and tissues with relatively high ATP demands, including the brain, heart, and skeletal muscle [38]. In particular, complex I deficiency is the most common cause of respiratory chain dysfunction [39]. Impairment of the ETC activity has also been observed not only in mitochondrial diseases, but also in Alzheimer's [40], Parkinson's disease [41], and in the ischemic/reperfused rat heart [42]. Moreover, complex III physically and functionally interacts with complexes I and IV [43], and its activity seems to have an influence on the other complexes [44, 45]. Taken together, my results further suggest that disorders and/or diseases associated with dysfunctional cytochrome segments, especially complex III [46] and IV [38], could potentially be alleviated by introduction of *Symplocarpus* AOX as gene therapy within human mitochondria.

In summary, data presented in the present study clearly show that *Symplocarpus* AOX, which plays a pivotal role in skunk cabbage heat production, confers cyanide resistance to human cells and prevents ROS production induced by AA exposure. Consequently, functional expression of *Symplocarpus* AOX seems to be a valuable tool for understanding not only the plant enzyme but also

the cytochrome pathway mutants associated with the human cell pathogenesis involved in tumorigenesis, apoptosis, and mitochondrial diseases.

Acknowledgements

This thesis would not have been completed without the help of many people to which I would like to say thank you. I wish to acknowledge the people who have contributed to the work presented in this thesis and also those who have contributed to my professional and personal development during the years as a PhD student.

I would like to express my gratitude to my main supervisor professor Kikukatsu Ito, for giving me an opportunity to work under his supervision and his enormous support at all time during the period of this project. His excellent teaching and coaching was always motivation and encouragement. I am also grateful for his strategic guidance and encouragement.

I would like to thank my co-supervisor professor Ken-ichi Tsutsumi, for his permanent encouragement, support, technical advice and for many valuable discussions.

I am grateful to my co-supervisor professor Wataru Mitsuhashi, for many helpful thoughts on my project.

I am also grateful to professor Yohtaro Katagata, for being my co-referee.

I would like to thank my colleagues in our laboratory, Yuka Ito, Yusuke Kakizaki, Takafumi Ogata, Akiko Tako, for their great cooperation.

I would also like to thank my former colleagues in our laboratory, Yoshihiko Onda, Takashi Kamata, Takanori Ito, Yoshiaki Kato, Minoru Otsuka,

Yukie Abe, Miyuki Morohashi, Megumi Ichikawa, for their assistance and encouragements.

I am thankful to my friends and colleagues in the Cryobiofrontier Research Center, Iwate University for their helpful collaboration.

REFERENCES

[1] McDonald, A.E. (2008) Alternative oxidase: an inter-kingdom perspective on the function and regulation of this broadly distributed 'cyanide-resistant' terminal oxidase. Func. Plant Biol. 35, 535-552.

[2] Wagner, A.M. and Moore, A.L. (1997) Structure and function of the plant alternative oxidase: its putative role in the oxygen defence mechanism. Biosci. Rep. 17, 319-333.

[3] Vanlerberghe, G.C. and McIntosh, L. (1997) Alternative oxidase: from gene to function. Annu. Rev. Plant Physiol. Plant Mol. Biol. 48, 703-734.

[4] Wagner, A.M., Krab, K., Wagner, M.J. and Moore, A.L. (2008) Regulation of thermogenesis in flowering Araceae: the role of the alternative oxidase. Biochim. Biophys. Acta 1777, 993-1000.

[5] Onda, Y., Kato, Y., Abe, Y., Ito, T., Morohashi, M., Ito, Y., Ichikawa, M., Matsukawa, K., Kakizaki, Y., Koiwa, H. and Ito, K. (2008) Functional coexpression of the mitochondrial alternative oxidase and uncoupling protein underlies thermoregulation in the thermogenic florets of skunk cabbage. Plant Physiol. 146, 636-645.

[6] Watling, J.R., Robinson, S.A. and Seymour, R.S. (2006) Contribution of the alternative pathway to respiration during thermogenesis in flowers of the sacred lotus. Plant Physiol. 140, 367-373.

[7] Maxwell, D.P., Wang, Y. and McIntosh, L. (1999) The alternative oxidase lowers mitochondrial reactive oxygen production in plant cells. Proc. Natl. Acad. Sci. USA 96, 8271-8276.

[8] Popov, V.N., Simonian, R.A., Skulachev, V.P. and Starkov, A.A. (1997) Inhibition of the alternative oxidase stimulates H_2O_2 production in plant mitochondria. FEBS Lett. 415, 87-90.

[9] Muller, F.L., Liu, Y. and Van Remmen, H. (2004) Complex III releases superoxide to both sides of the inner mitochondrial membrane. J. Biol. Chem. 279, 49064-49073.

[10] Turrens, J.F. (1997) Superoxide production by the mitochondrial respiratory chain. Biosci. Rep. 17, 3-8.

[11] Wallace, D.C. (1999) Mitochondrial diseases in man and mouse. Science 283, 1482-1488.

[12] Hüttemann, M., Lee, I., Samavati, L., Yu, H. and Doan, J.W. (2007) Regulation of mitochondrial oxidative phosphorylation through cell signaling. Biochim. Biophys. Acta 1773, 1701-1720.

[13] Hakkaart, G.A.J., Dassa, E.P., Jacobs, H.T. and Rustin, P. (2006) Allotopic expression of a mitochondrial alternative oxidase confers cyanide resistance to human cell respiration. EMBO Rep. 7, 341-345.

[14] Onda, Y., Kato, Y., Abe, Y., Ito, T., Ito-Inaba, Y., Morohashi, M., Ito, Y., Ichikawa, M., Matsukawa, K., Otsuka, M., Koiwa, H. and Ito, K. (2007) Pyruvate-sensitive AOX exists as a non-covalently associated dimer in the homeothermic spadix of the skunk cabbage, *Symplocarpus renifolius.* FEBS Lett. 581, 5852-5858.

[15] Elthon, T.E., Nickels, R.L. and McIntosh, L. (1989) Monoclonal antibodies to the alternative oxidase of higher plant mitochondria. Plant Physiol. 89, 1311-1317.

[16] Piva, T.J. and McEvoy-Bowe, E. (1998) Oxidation of glutaimine in HeLa cells: role and control of truncated TCA cycles in tumor mitochondria. J. Cell. Biochem. 68, 213-225.

[17] Matsukawa, K., Ogata, M., Hikage, T., Minami, H., Shimotai, Y., Saitoh, Y., Yamashita, T., Ouchi, A., Tsutsumi, R., Fujioka, T. and Tsutsumi, K. (2006) Antiproliferative activity of root extract from gentian plant (*Gentiana triflora*) on cultured and implanted tumor cells. Biosci. Biotechnol. Biochem. 70, 1046-1048.

[18] Duez, P., Kumps, A. and Mardens, Y. (1996) GC-MS profiling of urinary organic acids evaluated as a quantitative method. Clinical Chem. 42, 1609-1615.

[19] Rizzuto, R., Simpson, A.W., Brini, M. and Pozzan, T. (1992) Rapid changes of mitochondrial Ca^{2+} revealed by specific targeted recombinant aequorin. Nature 358, 325-327.

[20] Albury, M.S., Affourtit, C., Crichton, P.G. and Moore, A.L. (2002) Structure of the plant alternative oxidase. Site-directed mutagenesis provides new information on the active site and membrane topology. J. Biol. Chem. 277, 1190-1194.

[21] Affourtit, C., Albury, M.S., Crichton, P.G. and Moore, A.L. (2002) Exploring the molecular nature of alternative oxidase regulation and catalysis. FEBS Lett. 510, 121-126.

[22] Ajayi, W.U., Chaudhuri, M. and Hill G.C. (2002) Site-directed mutagenesis reveals the essentially of the conserved residues in the putative diiron active site of the trypanosome alternative oxidase. J. Biol.

Chem. 277, 8187-8193.

[23] Siedow, J.N. and Girvin, M.E. (1980) Alternative respiratory pathway: its role in seed respiration and its inhibition by propyl gallate. Plant Physiol. 65, 669-674.

[24] Umbach, A.L. and Siedow, J.N. (1993) Covalent and noncovalent dimers of the cyanide-resistant alternative oxidase protein in higher plant mitochondria and their relationship to enzyme activity. Plant Physiol. 103, 845-854.

[25] Umbach, A.L. and Siedow, J.N. (2000) The cyanide-resistant alternative oxidase from the fungi *Pichia stipitis* and *Neurospora crassa* are monomeric and lack regulatory features of the plant enzyme. Arch. Biochem. Biophys. 378, 234-245.

[26] Chaudhuri, M., Ott, R.D. and Hill, G.C. (2006) Trypanosome alternative oxidase: from molecule to function. Trends Parasitol. 22, 484-491.

[27] Jarmuszkiewicz, W., Czarna, M. and Sluse, F.E. (2005) Substrate kinetics of the *Acanthamoeba castellanii* alternative oxidase and the effects of GMP. Biochim. Biophys. Acta 1708, 71-78.

[28] Christofk, H.R., Vander Heiden, M.G., Harris, M.H., Ramanathan, A., Gerszten, R.E., Wei, R., Fleming, M.D., Schreiber, S.L. and Cantley, L.C. (2008) The M2 splice isoform of pyruvate kinase is important for cancer metabolism and tumor growth. Nature 452, 230-234.

[29] Nalvarte, I., Damdimopoulos, A.E. and Spyrou, G. (2004) Human mitochondrial thioredoxin reductase reduces cytochrome *c* and confers resistance to complex III inhibition. Free Rad. Biol. Med. 36, 1270-1278.

[30] Kim, K.M., Giedt, C.D., Basañez, G., O'Neill, J.W., Hill, J.J., Han, Y.H., Tzung, S.P., Zimmerberg, J., Hockenbery, D.M. and Zhang, K.Y. (2001) Biophysical characterization of recombinant human Bcl-2 and its interactions with an inhibitory ligand, antimycin A. Biochemistry 40, 4911-4922.

[31] Tzung, S.P., Kim, K.M., Basañez, G., Giedt, C.D., Simon, J., Zimmerberg, J., Zhang, K.Y. and Hockenbery, D.M. (2001) Antimycin A mimics a cell-death-inducing Bcl-2 homology domain 3. Nat. Cell. Biol. 3, 183-191.

[32] Hockenbery, D.M., Oltvai, Z.N., Yin, X.M., Milliman, C.L. and Korsmeyer, S.J. (1993) Bcl-2 functions in an antioxidant pathway to prevent apoptosis. Cell 75, 241-251.

[33] Gogvadze, V., Orrenius, S. and Zhivotovsky, B. (2008) Mitochondria in cancer cells: what is so special about them? Trends Cell Biol. 18, 165-173.

[34] Hoffmann, S., Spitkovsky, D., Radicella, J.P., Epe, B. and Wiesner, R.J. (2004) Reactive oxygen species derived from the mitochondrial respiratory chain are not responsible for the basal levels of oxidative base modifications observed in nuclear DNA of mammalian cells. Free Rad. Biol. Med. 36, 765-773.

[35] Oliveira, H.R., Curi, R. and Carpinelli, A.R. (1999) Glucose induces an acute increase of superoxide dismutase activity in incubated rat pancreatic islets. Am. J. Physiol. Cell Physiol. 276, 507-510.

[36] Desagher, S., Glowinski, J. and Prémont, J. (1997) Pyruvate protects neuron against hydrogen peroxide-induced toxicity. J. Neurosci. 17,

9060-9067.

[37] Townsend, D.M., Tew, K.D. and Tapiero, H. (2003) The importance of glutathione in human disease. Biomed. Pharmacother. 57, 145-155.

[38] Rötig, A., Lebon, S., Zinovieva, E., Mollet, J., Sarzi, E., Bonnefont, J.P. and Munnich, A. (2004) Molecular diagnostics of mitochondrial disorders. Biochim. Biophys. Acta 1659, 129-135.

[39] Lazarou, M., Thorburn, D.R., Ryan, M.T. and McKenzie, M. (2008) Assembly of mitochondrial complex I and defects in disease. Biochim. Biophys. Acta 1793, 78-88.

[40] Atamna, H. and Frey II, W.H. (2007) Mechanisms of mitochondrial dysfunction and energy deficiency in Alzhimer's disease. Mitochondrion 7, 297-310.

[41] Shults, C.W. (2004) Mitochondrial dysfunction and possible treatments in Parkinson's disease-a review. Mitochondrion 4, 641-648.

[42] Tompkins, A.J., Burwell, L.S., Digerness, S.B., Zaragoza, C., Holman, W.L. and Brookes, P.S. (2006) Mitochondrial dysfunction in cardiac ischemia-reperfusion injury: ROS from complex I, without inhibition. Biochim. Biophys. Acta 1762, 223-231.

[43] Genova, M.L., Baracca, A., Biondi, A., Casalena, G., Faccioli, M., Falasca, A.I., Formiggini, G., Sgarbi, G., Solaini, G. and Lenaz, G. (2008) Is supercomplex organization of the respiratory chain required for optimal electron transfer activity? Biochim. Biophys. Acta 1777, 740-746.

[44] Hargreaves, I.P., Duncan, A.J., Wu, L., Agrawal, A., Land, J.M. and Heales, S.J.R. (2007) Inhibition of mitochondrial complex IV leads to

secondary loss complex II-III activity: Implications for the pathogenesis and treatment of mitochondrial encephalomyopathies. Mitochondrion 7, 284-287.

[45] Paradies, G., Petrosillo, G., Pistolese, M. and Ruggiero, F.M. (2000) The effet of reactive oxygen species generated from the mitochondrial electron transport chain on the cytochrome *c* oxidase activity and on the cardiolipin content in bovine heart submitochondrial particles. FEBS Lett. 466, 323-326.

[46] Bénit, P., Lebon, S. and Rustin, P. (2008) Respiratory-chain diseases related to complex III deficiency. Biochim. Biophys. Acta 1793, 181-185.